

Lifetime predictions of prestressed concrete bridges—Evaluating parameters of relevance using Sobol' indices

David Sanio  | Mark Alexander Ahrens  | Peter Mark 

Institute of Concrete Structures, Ruhr-Universität Bochum, Bochum, Germany

Correspondence

David Sanio, Institute of Concrete Structures, Ruhr-Universität Bochum, Bochum, Germany.
 Email: david.sanio@rub.de

Abstract

The residual structural lifetime of concrete bridges is often limited by fatigue of the prestressing steel. In practice, numerical calculations of the structure are combined with Miner's rule—based on load frequencies and stress amplitudes—to estimate the damage. Thereby, various parameters must be accounted for whereof a few are actually relevant. Structural monitoring is valuable to increase the accuracy of lifetime predictions, but usually experts choose the right parameters on experience only. A more objective assessment can be reached by sensitivity analysis. A powerful method is provided by Sobol's variance-based indices. They quantify the influence of a single parameter's variance on the model's total variance and account for interactions in nonlinear models, too. Exemplified on a reference structure, sensitivity indices are determined. Meanwhile specific characteristics like the nonlinear behavior of concrete after cracking are considered. In this case, the key elements of lifetime prediction turn out to be the time-dependent losses of prestress and the traffic loads.

KEYWORDS

concrete bridges, fatigue, lifetime predictions, sensitivity analysis, Sobol' indices

1 | INTRODUCTION

Fatigue is commonly restrictive when predicting the residual lifetime of old and degraded concrete bridges.¹ However, it involves various uncertainties and enters significant scatter in forecasts.^{2–4} Structural monitoring of key parameters^{5–7} might extend the residual lifetime significantly by reducing the uncertainty of the input parameters of the prognosis.⁸ The crucial question concerns the choice of the right parameters to measure,⁹ which shall be answered by the results of this paper.

Especially for fatigue of prestressed concrete bridges under traffic, many parameters need to be incorporated into a complex numerical model.^{2,4} Since the bearing behavior of prestressed concrete is significantly nonlinear after cracking, the relevant parameters are not known beforehand. They may even change over time.⁹ To consider all these aspects, a comprehensive numerical model was developed, which is presented here.

While uncertainty analysis quantifies the variability of a model output based on uncertain input (e.g., References 10–12—results for lifetime predictions, e.g., see Reference 13)—sensitivity analysis methods were developed to identify the most relevant input parameters to the model output, or more precisely, to its variability.¹⁴ Conversely, also minor relevant parameters are identified, which affect the output only to a minor extend.¹⁵ To reduce computational cost in further evaluations, these parameters can be fixed to constant values. In this paper, a sensitivity analysis of a lifetime prediction model for concrete bridges is carried out to determine the important and less relevant parameters. Consequently, fixing less relevant parameters can be done based on the findings here.

There are many different methods available for sensitivity analyses, which involve varying computational costs. Starting from local derivative-based methods, nowadays global sensitivity analyses^{14,16} are to be preferred for complex and nonlinear models.¹⁷ Global

This is an open access article under the terms of the [Creative Commons Attribution](https://creativecommons.org/licenses/by/4.0/) License, which permits use, distribution and reproduction in any medium, provided the original work is properly cited.

©2021 Ernst & Sohn Verlag für Architektur und technische Wissenschaften GmbH & Co. KG, Berlin.

methods can be categorized into quantitative¹⁸ and qualitative¹⁹ ones. While the latter come along with a reduced computational cost, they should preferably be used to identify less relevant parameters, as it is possible with the elementary effect-method by Morris.^{19,20} An application of this to engineering structures and their lifetime predictions is given in Reference 21. In contrast, variance-based global sensitivity analyses are a powerful tool to quantify the individual impact of a parameter on the model output.¹⁸ One of the most sophisticated types are the variance-based sensitivity indices by Sobol',¹⁶ which are applied in the context of the work presented here to a complex computational model.

The objective of this paper is to determine the most relevant parameters in lifetime predictions of prestressed concrete bridges using sensitivity analysis methods. The selected method for this purpose is Sobol's variance-based sensitivity indices, which are outlined in Section 2. To consider as many different elements of prognosis as possible, a complex and comprehensive stochastic model for the lifetime prediction was developed, which comprises various uncertain parameters in the areas of loads, structure, time-dependent effects, material, and resistance. Section 3 describes the components of the modular model. Exemplified on a reference structure, some assumptions in the model were generalized to produce results which are valid for similar bridge types. For other bridge types, the model can be adapted but new sensitivity analyses are recommended. In Section 4, the results of the variance-based sensitivity indices are presented. For the computation, a new and improved approach for sampling is introduced, which was developed to increase the accuracy for a small sample size. Finally, conclusions are presented in Section 5.

2 | SENSITIVITY ANALYSIS METHOD

2.1 | Variance-based sensitivity indices

Variance-based sensitivity indices aim for analyzing complex models like nonlinear, nonmonotonic discontinuous systems.²² The impact of a model parameter X_i on the variability of the output Y can be quantified by analysis of variance (ANOVA) techniques. Therefore, the total variance of the output is decomposed into the variances of single parameters and into (co-)variances induced by correlation between the parameters. To assess the impact of the parameters, single parameters are fixed temporarily.

Let the model be a simple function of q input parameters X_i at first and assume all X_i are square-integrable. Thus, mathematically each parameter possesses a variance $V(X_i) < \infty$

$$Y = f(\mathbf{x}) = f(X_1, X_2, \dots, X_q). \quad (1)$$

The model spans a q -dimensional unit hyperspace Ω_q and can be split into 2^q components by ANOVA high-dimensional model representation.^{23,24} It comprises a single constant term of order zero f_0 , q linear terms f_i and q over 2 quadratic components f_{ij} , etc.

$$Y = f(\mathbf{x}) = f_0 + \sum_{i=1}^q f_i(X_i) + \sum_{i=1}^q \sum_{j>i}^q [f_{ij}(X_i, X_j) + \dots + f_{1,2,\dots,q}(X_1, X_2, \dots, X_q)]. \quad (2)$$

Indeed, decomposition is not unique, but Sobol'¹⁶ has proven all terms being orthogonal assuming all means but f_0 being zero. Thus, f_0 equals the expectation of Y

$$f_0 = E(Y). \quad (3)$$

Moreover, the higher order components are obtained from conditional expectations²³

$$f_i(X_i) = E(Y|X_i) - E(Y) = \int_0^1 \dots \int_0^1 f(\mathbf{x}) d\mathbf{x}_{-i} - f_0. \quad (4)$$

Therein, the index $-i$ denotes all dimensions but i , analogously $-[i,j]$ all dimensions but i and j

$$f_{ij}(X_i, X_j) = E(Y|X_i, X_j) - f_i - f_j - E(Y) = \int_0^1 \dots \int_0^1 f(\mathbf{x}) d\mathbf{x}_{-[i,j]} - f_i(X_i) - f_j(X_j) - f_0. \quad (5)$$

The total variance is gained by integration of the squared function

$$V(Y) = E(Y^2) - E(Y)^2 = \int_{\Omega_q} f^2(\mathbf{x}) d\mathbf{x} - f_0^2. \quad (6)$$

Due to orthogonality, the variance of Y can be decomposed analogously to Equation (2) into the input variances $V_i = V(f_i(X_i))$ and contributions due to parameter interaction V_{ij}

$$V(Y) = \sum_{i=1}^q V_i + \sum_{i=1}^q \sum_{j>i}^q [V_{ij} + \dots + V_{1,2,\dots,q}]. \quad (7)$$

Employing Equation (4), the variance due to a single parameter i follows to $V(f_i(X_i)) = V(E(Y|X_i))$. Related to the total variance, this directly leads to the first-order sensitivity indices S_i , also called direct effects, according to Sobol'¹⁶

$$S_i = \frac{V(f_i(X_i))}{V(Y)} = \frac{V(E(Y|X_i))}{V(Y)}. \quad (8)$$

Higher order sensitivity indices (S_{ij} up to $S_{1,2,\dots,q}$) can be obtained analogously if the parameter interaction $f_{ij}(X_i, X_j)$ is also considered.

From Equations (7) and (8), it follows that the sum of all 2^{q-1} sensitivity indices (all first and higher order ones) is always $\sum S_i = 1$. Moreover, in case of additive models, all first-order sensitivity indices always sum up to 1 while in nonadditive models, the sum might be smaller than 1, too. Then, the difference $1 - \sum S_i$ indicates the amount of interaction in the model.

The model's total variance $V(Y)$ can be expressed as the sum of conditional variances analog to Equation (7) and further variances. Again, the conditional variances are obtained fixing all parameters but X_i , while the further ones result from Y if X_i is fixed to x_i^*

simulation-wise. The result in nonlinear models might depend on the choice of x_i^* , too. For example, this is true for S-N-curves in fatigue lifetime estimations. So, the expected value of the conditional variances $V_{X-i}(Y|X_i = x_i^*)$ for all x_i^* employs $E_{X_i}(V_{X-i}(Y|X_i = x_i^*))$, in short $E(V(Y|X_{-i}))$. Finally, the total variance reads

$$V(Y) = V(E(Y|X_i)) + E(V(Y|X_i)) = V(E(Y|X_{-i})) + E(V(Y|X_{-i})). \quad (9)$$

Dividing Equation (9) by $V(Y)$ yields again the first-order index. Additionally, a second term for the variance due to interaction with other parameters is obtained. The latter one subtracted from 1 gives the total sensitivity index, also called total effect S_{Ti} ¹⁸

$$\begin{aligned} S_{Ti} &= 1 - \frac{V(E(Y|X_{-i}))}{V(Y)} \\ &= \frac{V_i + \sum_{j \neq i} V_{ij} + \sum_{j \neq i, k \neq i, k \neq j} \sum_{kk, k \neq i, k \neq j} V_{ijk} + \dots + V_{1,2,\dots,q}}{V(Y)} \\ &= S_i + \sum_{j \neq i} S_{ij} + \sum_{j \neq i, k \neq i, k \neq j} \sum_{kk, k \neq i, k \neq j} S_{ijk} + \dots + S_{1,2,\dots,q}. \end{aligned} \quad (10)$$

Thus, the total sensitivity index S_{Ti} additionally comprises all parameter interactions. Moreover, S_{Ti} is always greater than S_i . If S_{Ti} is close to S_i , interaction is of minor importance. For purely additive models, the sum of all parameters total sensitivity indices is 1, otherwise a value greater than 1.

2.2 | Numerical determination of variance-based sensitivity indices

Originally, Saltelli et al.¹⁴ presented an algorithm to compute both indices S_i and S_{Ti} efficiently. Later on, Glen and Isaacs²⁵ modified the method to compute the sensitivity indices from correlation coefficients. Due to their modification, the number of necessary simulations n was significantly lowered from n^2 to $n \cdot (q + 2)$, wherein q denotes the number of parameters involved in the model. More details can be found in Glen and Isaacs²⁵ and Saltelli et al.¹⁴

First, two independent matrices **A** and **B** both of size $(n \times q)$ must be generated by Monte-Carlo Sampling. For a practical implementation, Saltelli et al.¹⁸ recommend a single matrix with a doubled number of columns $(n \times 2 \cdot q)$ containing (quasi-)random numbers²⁶ and to generate the two matrices **A** and **B** thereof

$$\mathbf{A} = \begin{bmatrix} x_1^{(1)} & \dots & x_i^{(1)} & \dots & x_q^{(1)} \\ \vdots & \dots & \vdots & \dots & \vdots \\ x_1^{(n)} & \dots & x_i^{(n)} & \dots & x_q^{(n)} \end{bmatrix}; \mathbf{B} = \begin{bmatrix} x_{q+1}^{(1)} & \dots & x_{q+i}^{(1)} & \dots & x_{2q}^{(1)} \\ \vdots & \dots & \vdots & \dots & \vdots \\ x_{q+1}^{(n)} & \dots & x_{q+i}^{(n)} & \dots & x_{2q}^{(n)} \end{bmatrix}. \quad (11)$$

From both, q further matrices \mathbf{C}_i ($i = 1, 2, \dots, q$) are generated by substituting columns. While the i th column comes from **A**, all others columns come from **B**²⁷

$$\mathbf{C}_i = \begin{bmatrix} x_{q+1}^{(1)} & \dots & x_{q+i-1}^{(1)} & x_i^{(1)} & x_{q+i+1}^{(1)} & \dots & x_{2q}^{(1)} \\ \vdots & \dots & \vdots & \vdots & \vdots & \dots & \vdots \\ x_{q+1}^{(n)} & \dots & x_{q+i-1}^{(n)} & x_i^{(n)} & x_{q+i+1}^{(n)} & \dots & x_{2q}^{(n)} \end{bmatrix}. \quad (12)$$

For the parameter sets in **A**, **B**, and \mathbf{C}_i , the output by means of n -dimensional vectors **a**, **b**, and \mathbf{c}_i is obtained from model simulation. Altogether, $n \cdot (q + 2)$ simulation runs are necessary to gain the output. The first-order index S_i follows as Pearson's correlation coefficient between **a** and \mathbf{c}_i when all results Y of the model for the matrices **A** and **B** are used to get enhanced means μ_Y and variances σ_Y^2

$$S_i = \frac{1}{n-1} \sum_{m=1}^n \frac{(a_m - \mu_Y)(c_{i,m} - \mu_Y)}{\sigma_Y^2}. \quad (13)$$

Interpretation of an index determined from correlation is straightforward. Only in column i , **A** and \mathbf{C}_i possess equivalent values. Then, if X_i is significant for the output, the correlation between **a** and \mathbf{c}_i is high, else the sensitivity index is low. Similarly, the total sensitivity index S_{Ti} can be derived and interpreted. Since **B** and \mathbf{C}_i possess the same values for all entries but in column i (values of X_i), a high correlation (small S_{Ti} , see Equation 14) results if the impact of X_i is small

$$S_{Ti} = 1 - \frac{1}{n-1} \sum_{m=1}^n \frac{(b_m - \mu_Y)(c_{i,m} - \mu_Y)}{\sigma_Y^2}. \quad (14)$$

3 | NUMERICAL MODEL FOR LIFETIME PREDICTIONS OF CONCRETE BRIDGES

3.1 | Prediction model

To predict the structural lifetime of an aged prestressed concrete bridge under fatigue, a modular model is developed. This model comprises stochastic and time-dependent parameters. Some processes like creep even show both characteristics. To reduce the numerical effort, some parameters are idealized and simplified in advance. For example, time-dependent parameters are replaced by equivalent, deterministic, and scalable trends (see Section 3.3). They have been analyzed in advance and identified as minor relevant.²⁸ The single modules are presented separately in the subsequent sections.

As a representative application case, a degraded posttensioned prestressed concrete flyover in Düsseldorf, Germany serves as a reference structure (Figures 1 and 2). Built in 1959, it carried two traffic lanes over a total length of 302 m. The box girder has a constant height of 1.43 m, increasing web widths toward the support axes and a variable width toward the separating branches.

The prestressing consists of bar tendons (\emptyset 26 mm) made of high-strength steel St 80/105 ($f_{pk} = 1050 \text{ N/mm}^2$) and are placed in grouted metal-sheet ducts. Most of them run affine to the bending

moments induced by dead loads, only a few run straight in top- and bottom slab. From that time standard (DIN 4227²⁹), a maximum prestress of 307 kN per tendon can be expected.

At the joints, only a part of all tendons is coupled, which is nowadays standard but rarely done in those years. Due to threaded connections, coupling-joints are generally prone to fatigue and the more connections exist in a section, the higher the danger of fatigue is. Additionally, these construction joints often exhibit lowered tensile concrete strength, little reinforcement amounts, and tend to nonlinear stress distributions.³⁰

3.2 | Structure, loads, and stress calculation

For numerical computation of the structure, a finite element model of the bridge is set up. The hollow girder is discretized with linear beam elements. Columns, foundations, abutments, and the additional supports (steel columns near the coupling joints) are idealized by springs. Internal forces (bending moments and axial forces) are determined from a linear-elastic calculation. So, actions on the structure induced by dead-load, prestress, traffic, temperature, and settlements are all computed. The linear calculation is helpful to separate the finite element analysis from the stochastic evaluations on cross-sectional level.



FIGURE 1 Reference bridge at Düsseldorf, Germany. Source: David Sanio

In this way, uncertainty can be considered by scaling of the internal forces according to the variability of the loads.

On cross-sectional level, the nonlinear distribution of stresses has been computed on a layer model. Based on Bernoulli's hypothesis (plane-remains-plane) the strain gradient is iterated until equilibrium of internal and external forces is gained. To find the equilibrium, the Simplex-Algorithm³¹ is applied. Once knowing the strains, axial (N_R) and bending resistances (M_R) follow from Equations (15) and (16) by integration over the cross-sectional area A . Therein, the tendons resistance (index p) reflects the determinate part of the prestress

$$N_R = \int_A \sigma_c(z) dz + \sum_i \sigma_{s,i} \cdot A_{s,i} + \sum_j \sigma_{p,j} \cdot A_{p,j}, \quad (15)$$

$$M_R = \int_A \sigma_c(z) \cdot z dz + \sum_i \sigma_{s,i} \cdot A_{s,i} \cdot z_i + \sum_j \sigma_{p,j} \cdot A_{p,j} \cdot z_j. \quad (16)$$

The reinforcement is incorporated by five single rebar-layers (index s). Each one idealizes the reinforcement as a smeared layer in distinct position. For both, the prestressed tendons and the rebars, a linear-elastic behavior is assumed. This is true in case of high-cycle fatigue loads in typical frequencies ($n \gg 10^6$), where plastic deformation of rebar and tendons is generally disregarded.²⁸ In case of plastic deformation, fatigue failure would occur after only a few load-cycles (low cycle fatigue).

Resistance of concrete (index c) is activated for compression only (negative strains), while tensile stresses are assumed to be zero in the (precracked) coupling joint. Stresses are computed from a linear stress-strain curve according to Eurocode 2-2.³² The layer model allows the separation between different concrete classes in the top slab (B450 equivalent to a current C30/37) and the web and bottom slab (B300 equivalent to C20/25).

Stress ranges are caused by an alternating bending moment (ΔM) from cyclic loading by traffic. The mean stress comes from a basic bending moment (M_0), induced by permanent and quasi permanent loads. These loads comprise dead loads, slowly changing vertical

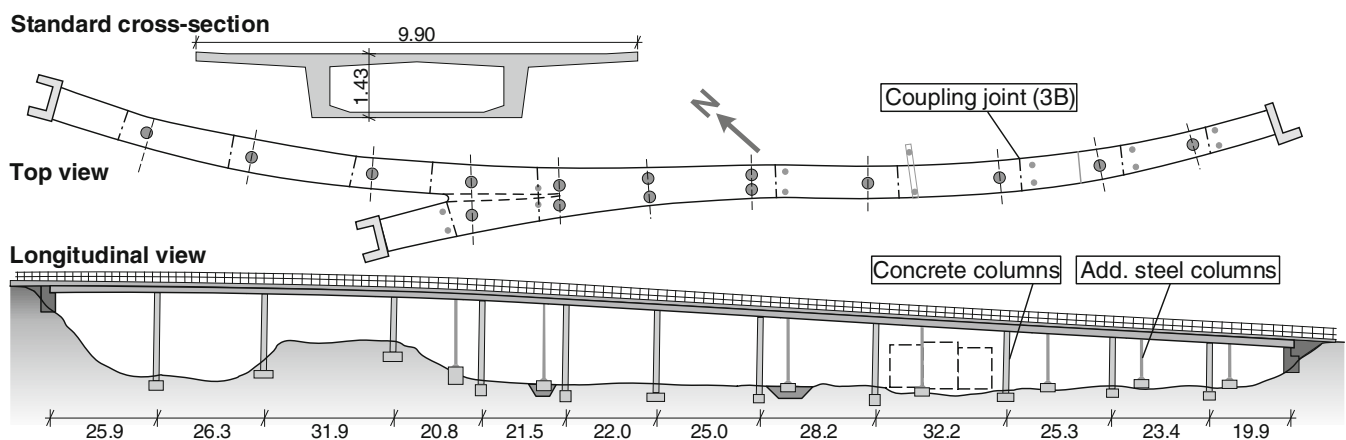


FIGURE 2 Top and longitudinal view of the reference structure. Source: David Sanio

temperature gradients (ΔT_i), settlement induced constraints (ΔS), and the indeterminate contribution of pre-stress (P').

Real traffic loads are very diverse for different bridges and difficult to implement accurately to a model. For simplification, the fatigue load model FLM 4 from Eurocode 1-2³³ has been employed, which distinguishes five truck types. These types vary from a small (2 axes 200 kN total load, 4.50 m length) to a heavy (5 axes 490 kN, 11.0 m), and a very long truck (5 axes, 450 kN, 14.1 m). Individual frequencies for each type depending on the road class are given in Eurocode 1-2 as well.

Alternating bending moments result from positioning the trucks from the FLM in the relevant load positions. Superposition with steady loads, temperature, settlements, and prestress delivers maximum and minimum bending moments (M_{\max} and M_{\min}). In a next step, stress amplitudes are obtained from the corresponding stresses and their difference ($\Delta\sigma = \sigma(M_{\max}) - \sigma(M_{\min})$). The stresses are evaluated at the representative coupling joint (3B in Figure 2).

3.3 | Time-dependent material behavior

Material properties of the steel practically do not change over time. Concrete exhibits posthardening that increases its strength and stiffness even after years. Based on the findings from Reference 28, the compressive strength of concrete f_c itself is minor relevant here. More important is Young's modulus E_c which is correlated to the strength. Thus, the compressive strength serves as a basic parameter to derive Young's modulus and its evolution over time (t) according to the formulas in Eurocode 2-2.³² The evolution of stiffness by posthardening $E_{cm}(t)$ is also taken from Eurocode 2-2 with f_{cm} as concrete mean compressive strength after 28 days and a parameter s which depends on the type of cement

$$E_{cm} = 22000 \left(\frac{f_{cm}}{10} \right)^{0.3}, \quad (17)$$

$$E_{cm}(t) = \left(\frac{f_{cm}(t)}{f_{cm}} \right)^{0.3} = \left(\frac{f_{cm} e^s [1 - \sqrt{28/t}]}{f_{cm}} \right)^{0.3}. \quad (18)$$

This time-dependent increase of the stiffness of the concrete changes the stress-state on cross-sectional level, overlaying with creep and shrinkage. This is accounted for via model B3, originally introduced by Bažant and Baweja.³⁴ The model gives a time-dependent increase of concrete strains which lowers the prestress in the tendons. Many different creep-and-shrinkage-curves with parameter variations were evaluated beforehand based on eight variable parameters (cf. Reference 28). The result is a stochastic process of the creep factor as presented in Figure 3, which is generated by different realizations of model B3. For simplification, a factor to govern the relative prestress losses with time has been derived thereof, which is considered in the simulations presented here. This factor reduces the

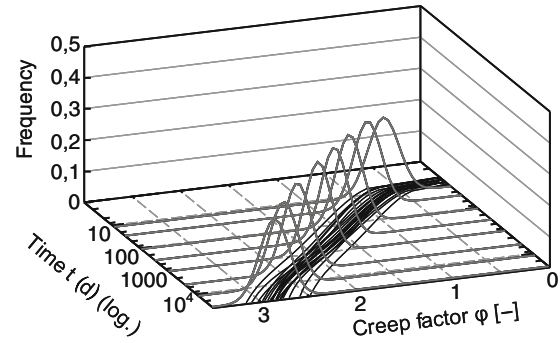


FIGURE 3 Evolution of creep factor as a stochastic process over time. Source: David Sanio

prestress as a nonlinear function of time. It is derived from the curves in Figure 3 as the mean.

3.4 | Lifetime prediction by damage accumulation

Damage assessment relies on the linear accumulation hypotheses according to Palmgren³⁵ and Miner.³⁶ Although some weaknesses are known for the model,^{37,38} it is still state of the art in lifecycle analysis of rebars and prestressed tendons in concrete. For this steel, the well-known double-logarithmic S-N-curve (Figure 4) relates stress amplitudes $\Delta\sigma$ to an expected number of cycles to failure N

$$\log N = \log N^* - k_{1/2} [\log \Delta\sigma - \log \Delta\sigma(N^*)]. \quad (19)$$

Dependent on the stress amplitude, two branches are defined by an inclination parameter $k_{1/2}$

$$k_{1/2} = \begin{cases} k_1 & \text{für } \Delta\sigma \geq \Delta\sigma(N^*) \\ k_2 & \text{für } \Delta\sigma < \Delta\sigma(N^*) \end{cases}. \quad (20)$$

Partial damage D_i is determined for different load levels i of $\Delta\sigma$ and accumulated according to Miner's rule

$$D = \sum_i D_i = \sum_i \frac{n(\Delta\sigma_i)}{N(\Delta\sigma_i)}. \quad (21)$$

Accumulation of all partial damages from erection at T_0 to the times associated with structural failure at $D = 1$ yields the structural lifetime T_F

$$\int_{T_0}^{T_F} D(t) dt = 1 \Rightarrow T_F. \quad (22)$$

During accumulation and due to nonlinearly evolving gradients of stress amplitudes and frequencies with time, the damage function $D(t)$ itself increases nonlinearly. To reduce computational efforts, the time-dependent model parameters are evaluated at discrete time instants.

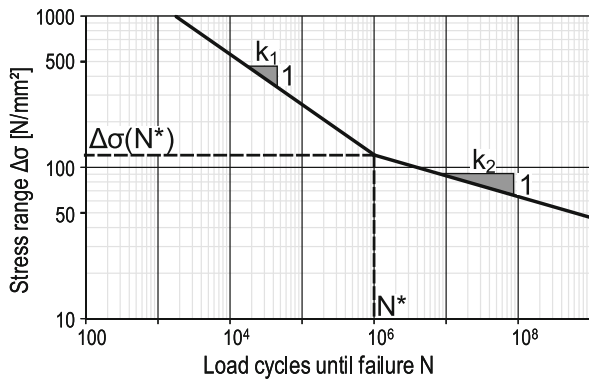


FIGURE 4 Typical S-N-curve for steel. Source: David Sanio

Precisely, a constant time interval of 10 years was used for the investigations here.

3.5 | Traffic frequencies

Since years, traffic amounts, frequencies, and weights are increasing worldwide. A trend expected to hold on in the future. In 2014, the German ministry for federal transport published a prognosis on the cargo amount (in tons · km) on German highways that is expected to grow by another 39% from 2010 to 2030.³⁹ By 2019, it had already increased by 19% according to data in Reference 40.

Thus and in consideration of the German guideline for recalculation of bridges,⁴¹ a continuous increase of traffic loads from the early 1950s was included in the model; also to account for formerly lower traffic loads on the roads at the time of erection of the bridge.³⁰ For simplification, a linear increase of heavy weight traffic by 15.000 trucks (=2%) per year was implemented.

3.6 | Stochastic analysis of structural lifetime subjected to fatigue

The fatigue lifetime forecast from stochastic simulation considering all uncertain model parameters by means of accumulated damages over time is shown in Figures 5 and 6. All parameters have been generated uncorrelated by Latin-Hypercube Sampling according to the distribution characteristics listed in Table 1. The impact of correlations between the input parameters was analyzed in depth by Sanio et al.¹³

The stochastic forecast bases on 200 simulations of the fatigue lifetime. Due to time-dependent effects (e.g., creep, shrinkage, concrete hardening, traffic amounts, and frequencies), these simulations comprise a multitude of individual damage computations. Time is discretized in 10 years intervals (see Section 3.4) up to a maximum of 200 years. The initial traffic amount was set to $3.5 \cdot 10^6$ trucks per year. For each time-step, the relevant temperature gradients ΔT_i were accounted for Reference 42, which were idealized as inner constraints

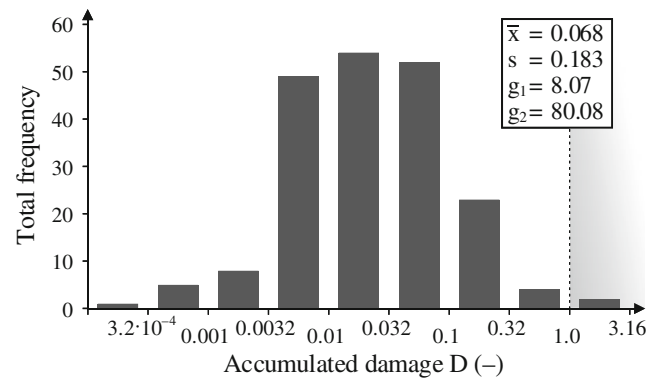


FIGURE 5 Histogram of accumulated damage D. Source: David Sanio

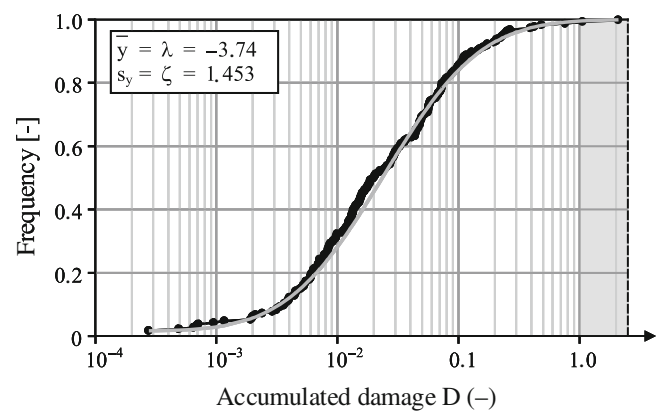


FIGURE 6 Empirical and fitted CDF's of log-normal type. Source: David Sanio

in corresponding frequencies.⁹ In total, five relevant temperature gradients were combined to five truck-loads defined in FLM 4. Each stress-amplitude results from the stress-difference at the upper and lower load level. Thus, stresses in the tendons are computed 1000 times per entire lifetime simulation (20 time-steps, five temperature gradients per time-step, five truck types per temperature gradient, two stress levels per truck and stress range).

The histogram of accumulated damages obtained from simulation is shown in Figure 5. The empirical cumulative density function is given in Figure 6. The region of fatigue failure ($D \geq 1$) is gray-shaded. Due to logarithmic scaling and supported by the higher order moments distribution's skewness ($g_1 > 0$) and kurtosis ($g_2 > 0$) become obvious. Kurtosis indicates a comparatively flatter distribution with heavy tails.

Goodness of fit testing employing Kolmogorov-Smirnov's statistic supports a log-normal distribution of data (gray in Figure 6) on a significance level $\alpha = .05\%$ while Anderson-Darling's more powerful test rejects the hypothesis. Other distribution functions like the Weibull's one cannot be established at all. Thus, due to lack of evidence, the total damage is assumed log-normally distributed in the remainder.

TABLE 1 Distribution parameters for the model

	Parameter i	μ_i	σ_i	Distribution
Prestressing steel	Prestrain $\varepsilon_p^{(0)}$ (%)	2.175	0.1	$N(\mu; \sigma)$
	Cross-sectional area of tendons $A_{p,i}$ (cm ²)	26.55	0.424	$N(\mu; \sigma)$
	Slope of S - N -curve k_2 (–)	7.0	0.5	$LN(\lambda; \zeta)$
	Loss of pre-stress (creep/shrinkage) a_{C+S} (–)	1.0	0.1	$N(\mu; \sigma)$
Concrete	Concrete strength of web and bottom slab $f_{c,w+bs}$ (N/mm ²)	38.0	5.0	$LN(\lambda; \zeta)$
	Concrete strength of deck slab $f_{c,ds}$ (N/mm ²)	45.0	5.0	$LN(\lambda; \zeta)$
	Cement-dependent parameter for hardening s (–)	0.38	0.038	$N(\mu; \sigma)$
Geometry	Geometry via deck slab width b_{ds} (m)	4.95	0.50	$N(\mu; \sigma)$
	Vertical position of the tendon z'_{p1} (m)	1.31	0.01	$N(\mu; \sigma)$
	Position of the coupling joint x_{cj} (m)	–	0.1	$N(\mu; \sigma)$
Loads	Increase of traffic density dn/dt	15 000	5000	$N(\mu; \sigma)$
	Weight of trucks from FLM4 (scaled) w_2 to w_4 (–)	1.0	0.10	$N(\mu; \sigma)$
	Temperature gradient: ΔT (–4 to –8 K)	1.0	0.20	$N(\mu; \sigma)$

4 | COMPUTATION OF SENSITIVITY INDICES AND RESULTS

4.1 | General remarks

Sensitivity indices based on correlation coefficients follow from Equations (13) and (14). While the first-order index S_i quantifies just the direct impact of a parameter's variance $V(X_i)$ on the variance of the output $V(Y)$, the total index S_{Ti} also includes covariances regarding parameter interaction (e.g., $V(X_i, X_j)$ or $V(X_i, X_j, X_k)$).

For analysis of the lifetime prediction model of the reference structure, 100 lifetime simulations have been performed. Nineteen parameters are involved in the model $(19 + 2) \cdot 100 = 2100$ simulations of damages accumulated after 200 years were already necessary.¹⁴ Inclusion of covariances and higher order sensitivity indices as well as an improved convergence behavior are all linked to more simulations that have been waived due to the associated numerical effort. Thus, the results for the reference structure exemplify the general concept but are only conditionally universal. Nevertheless, they may serve as representative benchmarks for similar structures and provide guidance for others. As it is shown in Reference 28, greater numbers of simulation are recommended.

4.2 | Sampling

The sample sets for model simulation are generated by drawing samples from stochastic populations. Thereby, the input of each parameter is limited by intervals according to its associated distribution function. Each simulation employs distinct datasets, so-called realizations. In this way, an originally continuous distribution function is discretized by a fixed number of realizations. In literature, a variety of alternative methods for sampling exists.^{14,43} Besides random sampling, also known as Monte-Carlo Sampling, enhanced methods like

Latin Hypercube sampling a derivative of the efficient stratified sampling methods are well established.

The fundamental idea of all sampling methods is the same and independent from the distribution being sampled. By inversion of the distribution function $F^{-1}(y)$, samples x_i are generated

$$F(x) = y \Leftrightarrow x = F^{-1}(y). \quad (23)$$

A mathematically invertible distribution function is prerequisite (which is practically not an issue), otherwise special procedures must be employed that are not addressed here.

First, uniformly distributed data is sampled between the limits zero and one ($0 < y < 1$). Thereof, several values n_{sim} are picked and used as input with an inverted distribution function to gain samples with desired properties X_i . The only difference of all alternative sampling methods concerns the order of data being picked from the uniform interval $[0; 1]$ and how realizations are combined to form a set if q variables are involved in the procedure. Besides, in case of Latin Hypercube sampling employing the midpoint approach, the only random element concerns the order of permutation

$$x_j = [x_{j1}, x_{j2}, \dots, x_{jq}], \quad j = 1, 2, \dots, n. \quad (24)$$

Computation of sensitivity indices rests on two independent matrices \mathbf{A} and \mathbf{B} , both containing n realizations of all q parameters. As already discussed in greater detail in Section 2.2, the indices are obtained from result vectors of combined matrices \mathbf{C}_i and the original matrices \mathbf{A} and \mathbf{B} . Fundamental is the independency of \mathbf{A} and \mathbf{B} , since spurious correlation might occur and impair the sensitivity indices otherwise.²⁵

Saltelli et al.¹⁴ propose to generate a joint matrix of random numbers of the size $(2n \times q)$ by using a random sampling, see Figure 7A). Afterward, it is split in half and realizations for \mathbf{A} and \mathbf{B} are generated.

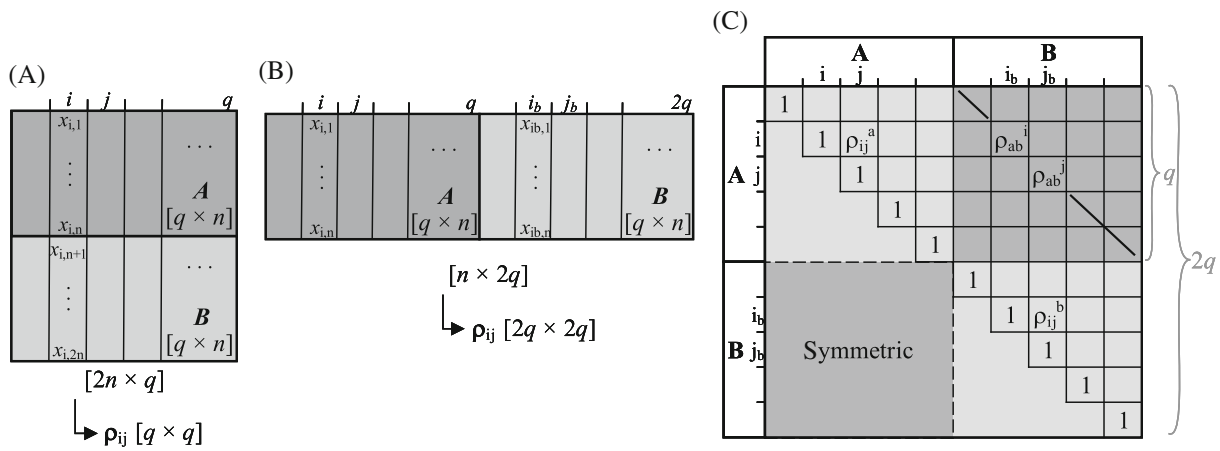


FIGURE 7 Dimensions and combinations of the two sample matrices **A** and **B** (top); correlation matrix in case of modified sampling (bottom). A, Original sampling. B, Modified sampling. C, Correlation matrix. Source: David Sanio

So, both matrices are independent. Sobol'¹⁶ specifically proposes to use a random sampling based on quasi-random numbers.

The proposed modification involves a sampling with correlation control and iterative adaption among the input. It aims at zero correlation as granted by the unity matrix. The whole procedure of a sampling with correlation control has been introduced by Iman and Conover.⁴⁴ Its principal idea is to change the entries within each column of the sampling matrix (here: size $[n \times 2q]$, Figure 7B) until the target correlation is reached. Therefore, Cholesky decomposition, the inverse standard-normal distribution and an auxiliary matrix are necessary to iteratively approximate the target correlation. A detailed description is presented by Helton and Davis.⁴⁵ The proposed sampling approach is briefly summarized in its key elements in the remainder.

All q columns of matrix **A** contain realizations of the basic model parameters X_i by Latin Hypercube sampling. Next, the realizations in **B** are added as q further but independent basic parameters X'_i as shown in light gray in Figure 7B). This ends up with a matrix $(n \times 2q)$ and an associated correlation matrix with a doubled number of entries $(2q \times 2q)$; cf. Figure 7C). Here, the new correlation matrix still contains the two original correlation matrices at the upper left and lower right quadrants along its main diagonal. Added superscripts a and b on the symbol of the correlation coefficient ρ_{ij} index the associated matrices **A** and **B**, respectively. The dark-gray-shaded quadrants aside the main diagonal of the correlation matrix include the correlation coefficients between the two matrices **A** and **B**. Entries along the secondary diagonals capture the correlation between the basic variables X_i and X'_i from **A** and **B**. They quantify the de facto dependency of the two matrices which is at best zero to grant unaffected result vectors a and b .

The sampling procedure with correlation control is applied to the matrix in Figure 7B). A target correlation matrix is defined, with the previously described entries to be zero for independence. By repeating the procedure, the correlation was reduced to values <0.01 for independent input.

4.3 | Results of sensitivity analyses

All sensitivity indices for the 19 model parameters according to Table 1 are summarized in Figures 8 and 9. The first-order index in the pie-chart (Figure 8A) presents the direct impact of all parameters on the scatter of the response. The scaling factor of time-dependent prestress losses ($S_{aC+S} = 0.15$), the exact location of the coupling joint ($S_{xcj} = 0.05$), and the load from truck type no. 3 of FLM 4 ($S_{w3} = 0.26$) shows the greatest impact on the model uncertainty. By definition, the sum of all S_i is always smaller than 1 ($\sum S_i \leq 1$) and exactly 1 for purely additive models,¹⁴ while here it yields $\sum S_i = 0.49$. Thus, relevant interaction among parameters must be expected.

Besides simple variances $V(X_i)$, total sensitivity indices S_{Ti} (Figure 8B) cover the impact of all covariances and thus parameter interactions, too. They reflect the total impact of parameters on a model. Besides the three parameters above ($S_{T,w3} = 0.70$, $S_{T,aC+S} = 0.53$, $S_{T,xcj} = 0.30$), the yearly increase of traffic amounts dn/dt turns out being important ($S_{T,n} = 0.27$). Other parameters do not impair the result significantly. The sum of all total sensitivities yields $\sum S_{Ti} = 1.93$. Compared to $\sum S_{Ti} = 1$ for purely additive models, this indicates significant parameter interactions again.

Finally, the difference of total and simple sensitivity indices ($S_{Ti} - S_i$, Figure 8C) is discussed. It quantifies the interaction of parameters only. The above-identified parameters are supposed to interact meaningful while others do not contribute considerably.

Stable results require a great number of simulations, especially if the sensitivity indices are small or even close to the range of spurious correlation. For the results presented in this paper, some indices close to zero were found to take on negative values as well. Since this is factually not possible, these results were set to zero. Due to immense computational costs linked with the lifetime-model from Section 3, the convergence behavior for numerically determined sensitivity indices was assessed on simplified model with less computational cost and fewer parameters. Details can be found in Reference 28. For stable and reliable results, at least 1000 simulations are recommended.

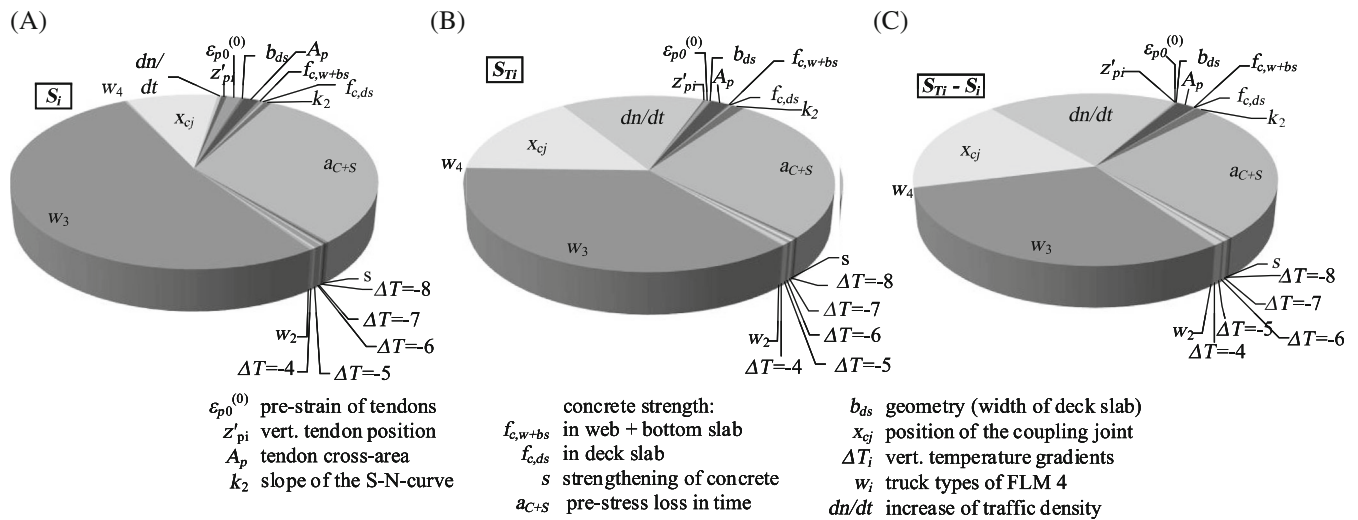


FIGURE 8 First-order S_i (top) and total sensitivity indices S_{T_i} (bottom left) along with quantified interactions (bottom right). Source: David Sanio

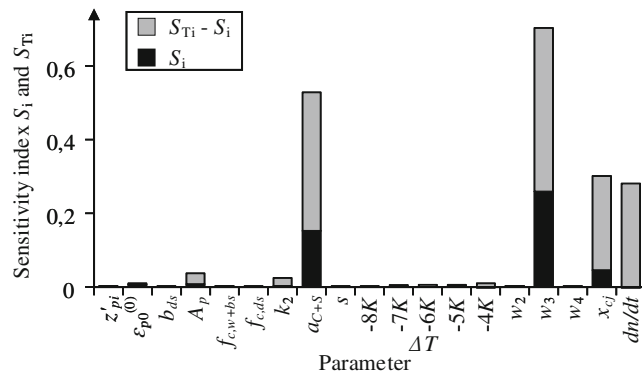


FIGURE 9 First-order (S_i) and total sensitivity indices (S_{T_i}). Source: David Sanio

5 | CONCLUSIONS

In this paper, variance-based sensitivity indices, also known as Sobol' indices, are determined to assess the sources of uncertainty of fatigue lifetime predictions of prestressed concrete bridges. The comprehensive model processes linear-elastic and nonlinear bearing behavior and stresses in the prestressing steel due to concrete cracking, idealized traffic loads from codes superposed with temperature-induced constraints, as well as time-dependent prestress losses. Fatigue damage is captured by the S - N -approach and linear accumulation. For all parameters, distribution functions of their variance were defined. This is also true for geometric and material parameters, which govern structural resistance.

From the results of the sensitivity analysis, a few leading parameters were identified which significantly affect the variance of the model output. They are the key elements to more accurate lifetime predictions of prestressed concrete bridges under fatigue. To improve the predictions, their uncertainty must be reduced, for example by means of monitoring: The most important elements are as follows.

1. traffic loads, which were represented by a truck from the fatigue load model 4 according to the Eurocodes;
2. the loss of prestress due to creep and shrinkage, which was incorporated by the time-dependent model B3 and which increases the frequency of concrete cracking;
3. the traffic frequency, which was incorporated by an annually incrementing function in accordance with the global trend of growing traffic amounts; and
4. the exact position of the coupling joint, which is the design point of the structural model as it is a well-known weak point of aged bridges.

In particular, the first two elements interact strongly with other parameters by means of covariances, as it can be seen from the sensitivity indices ($S_{T_i} - S_i \gg 0$). This is led back to a significantly altered bearing behavior if concrete cracks under higher loads. This means that reducing the variance of one of these parameters would have a greater-than-linear effect on the reduction of the variance of the model output. The latter two are dominating with their direct linear influence on the output, which is given by the first order sensitivity index ($S_i \gg 0$). Other parameters, for example, the compressive strength and Young's modulus of concrete, are identified almost irrelevant here.

Stable results require a great number of simulations, especially if sensitivity indices are close to zero. For a reliable quantitative evaluation, especially with regard to the minor relevant parameters, further simulations ($n > 1000$) are required. Nevertheless, the results show a tendency and are qualitatively true for the most relevant parameters.

The results correspond to the experience gained in engineering practice. Here, the proposed method helps to quantify the knowledge from experience. The results were determined for a prestressed concrete bridge with box girder cross section and medium span length as continuous girders. For other structures and other models, the presented method helps to perform a similar quantitative evaluation in advance.

In practice, the uncertainty of the governing parameters can be reduced by on-site measurements. In particular, the following monitoring measures are recommended to be monitored.

1. Traffic loads obviously have a considerable potential for increasing the accuracy, since they are incorporated into the calculation by means of conservative load models. Real loads can be measured for the current condition—for example, by weigh in motion systems or direct strain measurements, cf. Reference 30.
2. The frequency of the transition of the cross section to the cracked state due to decreasing prestress and increasing loads can be determined by crack widths measurement. Combined with corresponding temperature or traffic loads, the model can be calibrated.
3. Regarding the load frequency, accurate load histories often can be estimated from traffic counts on-site or nearby. So, even retrospective evaluations are possible. They can also serve as a basis for predicting load frequencies.
4. The accuracy of the structural model can be significantly increased with comparatively little effort by a 3D digital survey of the structure—for example, by means of laser scans, cf. Reference 8.

Finally, it can be concluded that especially measurements of the right elements can reduce uncertainty in the prediction of structural lifetime significantly. The most relevant parameters were identified in this paper for a real reference structure. The results serve as a basis for experts' decisions on the right elements for a structural monitoring, some elements are given. The quantitative evaluation of this gain in accuracy through measurements is part of further investigations.²⁸ An approach by the authors will be published soon.

DATA AVAILABILITY STATEMENT

The data that support the findings of this study are available from the corresponding author upon reasonable request.

ORCID

David Sanio  <https://orcid.org/0000-0002-2507-3578>

Mark Alexander Ahrens  <https://orcid.org/0000-0002-2337-1571>

Peter Mark  <https://orcid.org/0000-0003-1812-2148>

REFERENCES

1. Ahrens MA, Mark P. Lifetime simulation of concrete structures stochastically based time-dependent analyses applied to a degraded arch bridge. *Beton-und Stahlbetonbau*. 2011;106(4):220–230. <https://doi.org/10.1002/best.201000092>.
2. Ahrens MA. Precision-assessment of lifetime prognoses based on SN-approaches of RC-structures exposed to fatigue loads. In: Strauss A, Frangopol D, Bergmeister K, editors. *Life-cycle and sustainability of civil infrastructure systems*. Proceedings of the 3rd International Symposium on Life-Cycle Civil Engineering (IALCCE). Hoboken, NJ: CRC Press, 2012; p. 109.
3. Gao R, Li J, Ang AH-S. Stochastic analysis of fatigue of concrete bridges. *Struct Infrastruct Eng*. 2019;15(7):925–939. <https://doi.org/10.1080/15732479.2019.1569073>.
4. Crespo-Minguillón C, Casas JR. Fatigue reliability analysis of prestressed concrete bridges. *J Struct Eng*. 1998;124(12):1458–1466. [https://doi.org/10.1061/\(ASCE\)0733-9445\(1998\)124:12\(1458\)](https://doi.org/10.1061/(ASCE)0733-9445(1998)124:12(1458)).
5. Rodrigues C, Félix C, Lage A, Figueiras J. Development of a long-term monitoring system based on FBG sensors applied to concrete bridges. *Eng Struct*. 2010;32(8):1993–2002. <https://doi.org/10.1016/j.engstruct.2010.02.033>.
6. Nair A, Cai CS. Acoustic emission monitoring of bridges: Review and case studies. *Eng Struct*. 2010;32(6):1704–1714. <https://doi.org/10.1016/j.engstruct.2010.02.020>.
7. Bień J, Kuźawa M, Kamiński T. Strategies and tools for the monitoring of concrete bridges. *Struct Concrete*. 2020;21(4):1227–1239. <https://doi.org/10.1002/suco.201900410>.
8. Sanio D, Löschmann J, Mark P, Ahrens MA. Measurements vs. analytical methods to evaluate fatigue of tendons in concrete bridges. *Bautechnik*. 2018;95(2):99–110. <https://doi.org/10.1002/bate.201700092>.
9. Sanio D, Ahrens MA. Identification of relevant but stochastic input parameters for fatigue assessment of pre-stressed concrete bridges by monitoring. In: Papadrakakis M, Papadopoulos V, Stefanou G, editors. *Proceedings of the 1st International Conference on Uncertainty Quantification in Computational Sciences and Engineering*. ECCOMAS Thematic Conference, Greece: National Technical University of Athens, 2015; p. 947–960. <https://doi.org/10.7712/120215.4319.712>.
10. Walpole RE, Myers RH, Myers SL, Ye K. *Probability & statistics for engineers & scientists*. 9th ed. Boston, MA: Prentice Hall, 2012.
11. Ang AH-S, Tang WH. *Probability concepts in engineering*. Emphasis on applications in civil & environmental engineering. 2nd ed. Hoboken, NJ: Wiley, 2007.
12. Augusti G, Baratta A, Casciati F. *Probabilistic methods in structural engineering*. Boca Raton, FL: Chapman and Hall/CRC, 2014.
13. Sanio D, Ahrens MA, Mark P. Tackling uncertainty in structural lifetime evaluations. Assessment of the impact of monitoring data and correlated input parameters on a prognosis. *Beton-und Stahlbetonbau*. 2018;113(S2):48–54. <https://doi.org/10.1002/best.201800036>.
14. Saltelli A, Ratto M, Andres T, et al. *Global sensitivity analysis*. The primer. Chichester: John Wiley & Sons, 2008.
15. Saltelli A, Tarantola S. On the relative importance of input factors in mathematical models. *J Am Stat Assoc*. 2002;97(459):702–709. <https://doi.org/10.1198/016214502388618447>.
16. Sobol I. Global sensitivity indices for nonlinear mathematical models and their Monte Carlo estimates. *Math Comput Simul*. 2001;55(1–3):271–280. [https://doi.org/10.1016/S0378-4754\(00\)00270-6](https://doi.org/10.1016/S0378-4754(00)00270-6).
17. Wainwright HM, Finsterle S, Jung Y, Zhou Q, Birkholzer JT. Making sense of global sensitivity analyses. *Comput Geosci*. 2014;65:84–94. <https://doi.org/10.1016/j.cageo.2013.06.006>.
18. Saltelli A, Annoni P, Azzini I, Campolongo F, Ratto M, Tarantola S. Variance based sensitivity analysis of model output. Design and estimator for the total sensitivity index. *Comput Phys Commun*. 2010;181(2):259–270. <https://doi.org/10.1016/j.cpc.2009.09.018>.
19. Morris MD. Factorial sampling plans for preliminary computational experiments. *Dent Tech*. 1991;33(2):161–174. <https://doi.org/10.2307/1269043>.
20. Campolongo F, Cariboni J, Saltelli A. An effective screening design for sensitivity analysis of large models. *Environ Model Softw*. 2007;22(10):1509–1518. <https://doi.org/10.1016/j.envsoft.2006.10.004>.
21. Sanio D, Obel M, Mark P. Screening methods to reduce complex models of existing structures. In: Yurchenko D, Proske D, editors. *Proceedings of 17th International Probabilistic Workshop (IPW)*, Heriot-Watt University; Edinburgh, 2019; p. 51–56.
22. Iooss B, Lemaitre P. A review on global sensitivity analysis methods: A review on global sensitivity analysis methods. In: Dellino G, Meloni C, editors. *Uncertainty management in simulation-*

- optimization of complex systems. Algorithms and applications. Boston: Springer, 2015; p. 101–122.
23. Archer GEB, Saltelli A, Sobol IM. Sensitivity measures, ANOVA-like techniques and the use of bootstrap. *J Statist Comput Simul.* 1997; 58(2):99–120. <https://doi.org/10.1080/00949659708811825>.
 24. Sobol IM. Theorems and examples on high dimensional model representation. *Rel Eng Syst Saf.* 2003;79(2):187–193. [https://doi.org/10.1016/S0951-8320\(02\)00229-6](https://doi.org/10.1016/S0951-8320(02)00229-6).
 25. Glen G, Isaacs K. Estimating Sobol sensitivity indices using correlations. *Environ Model Softw.* 2012;37:157–166. <https://doi.org/10.1016/j.envsoft.2012.03.014>.
 26. Sobol IM. Uniformly distributed sequences with an additional uniform property. *USSR Comput Math Math Phys.* 1976;16(5):236–242. [https://doi.org/10.1016/0041-5553\(76\)90154-3](https://doi.org/10.1016/0041-5553(76)90154-3).
 27. Saltelli A. Making best use of model evaluations to compute sensitivity indices. *Comput Phys Commun.* 2002;145(2):280–297. [https://doi.org/10.1016/S0010-4655\(02\)00280-1](https://doi.org/10.1016/S0010-4655(02)00280-1).
 28. Sanio D. Accuracy of monitoring-based lifetime-predictions for prestressed concrete bridges prone to fatigue [PhD thesis]. Bochum: Schriftenreihe des Instituts für Konstruktiven Ingenieurbau; 2017.
 29. DIN—Deutsches Institut für Normung e.V. DIN 4227, Spannbeton. Berlin: Beuth Verlag, 1953.
 30. Sanio D, Ahrens MA, Mark P. Detecting the limits of accuracy of lifetime predictions by structural monitoring. In: Chen A, Frangopol DM, editors. *Bridge maintenance, safety, management and life extension. Proceedings of the 7th International Conference of Bridge Maintenance, Safety and Management.* Boca Raton: CRC Press, 2014; p. 416–423.
 31. Nelder JA, Mead R. A simplex method for function minimization. *Comput J.* 1965;7(4):308–313. <https://doi.org/10.1093/comjnl/7.4.308>.
 32. EN 1992-2, *Eurocode 2: Design of concrete structures*, 2010.
 33. EN 1991-2, *Eurocode 1: Actions on structures*, 2010.
 34. Bažant ZP, Baweja S. Creep and shrinkage prediction model for analysis and design of concrete structures – Model B3. *Mater Struct.* 1995;28(6):357–365. <https://doi.org/10.1007/BF02473152>.
 35. Pålmgren A. Die Lebensdauer von Kugellagern. *Zeitschrift des Vereins Deutscher Ingenieure.* 1924;68(14):339–341.
 36. Miner MA. Cumulative damage in fatigue. *J Appl Mech.* 1945;12(3): 159–164.
 37. Schütz W. A history of fatigue. *Eng Fracture Mech.* 1996;54(2): 263–300. [https://doi.org/10.1016/0013-7944\(95\)00178-6](https://doi.org/10.1016/0013-7944(95)00178-6).
 38. Schijve J. Fatigue of structures and materials in the 20th century and the state of the art. *Int J Fatigue.* 2003;25(8):679–702. [https://doi.org/10.1016/S0142-1123\(03\)00051-3](https://doi.org/10.1016/S0142-1123(03)00051-3).
 39. Schubert M, Kluth T, Nebauer G, et al. *Verkehrsverflechtungsprognose 2030*, 2014.
 40. BMVI. *Gleitende Mittelfristprognose für den Güter- und Personenverkehr. Mittelfristprognose Sommer 2020.* München, 2020.
 41. BMVBS. *Richtlinie zur Nachrechnung von Straßenbrücken im Bestand (Nachrechnungsrichtlinien)*, 2011.
 42. Sanio D, Mark P, Ahrens MA. Computation of temperature fields on bridges. Implementation by means of spread-sheets. *Beton- und Stahlbetonbau.* 2017;112(2):85–95. <https://doi.org/10.1002/best.201600068>.
 43. Roos D, Adam U, Bayer V. Design reliability analysis. In: *24th CAD-FEM Users' Meeting. International Congress on FEM Technology*, 2006.
 44. Iman RL, Conover WJ. A distribution-free approach to inducing rank correlation among input variables. *Commun Statist—Simul Comput.* 1982; 11(3):311–334. <https://doi.org/10.1080/03610918208812265>.
 45. Helton JC, Davis FJ. Latin hypercube sampling and the propagation of uncertainty in analyses of complex systems. *Rel Eng Syst Saf.* 2003; 81(1):23–69. [https://doi.org/10.1016/S0951-8320\(03\)00058-9](https://doi.org/10.1016/S0951-8320(03)00058-9).

How to cite this article: Sanio D, Ahrens MA, Mark P. Lifetime predictions of prestressed concrete bridges—Evaluating parameters of relevance using Sobol' indices. *Civil Engineering Design.* 2022;4:143–53. <https://doi.org/10.1002/cend.202100009>